Supporting Information (SI)

Sulfur, nitrogen dual-doped porous graphene nanohybrid for ultraselective Hg(II) separation over Pb(II) and Cu(II)

Hua Tian, [a] Jianrong Guo, [a,b] Zili Pang, [a] Minghua Hu [a,b] and Junhui He, [*,a]

[a] *Functional Nanomaterials Laboratory, Center for Micro/Nanomaterials and Technology, and Key Laboratory of Photochemical Conversion and Optoelectronic Materials, Technical Institute of Physics and Chemistry, Chinese Academy of Sciences, Beijing, 100190, China*

[b] *University of Chinese Academy of Sciences, No.19(A) Yuquan Road, Shijingshan District, Beijing, 100049, China*

Email: jhhe@mail.ipc.ac.cn

Experimental section

Chemicals. All reagents in this study were obtained from commercial suppliers and used as received unless otherwise noted. Aqueous solutions were prepared using ultrapure water obtained through a three-stage Millipore Mill-Q Plus 185 purification system.

Synthesis of SNPG nanohybrid. Graphene oxide (GO) was synthesized from natural graphite according to modified Hummers' method.[1] SNPG was prepared as follow: 1.2 mL $(NH_4)_2S$ and 50 μL (3-Mercaptopropyl) trimethoxysilane (MPTS) were dispersed into 10 mL of GO (2 mg mL^{-1}, in water) in a glass bottle at room temperature. Afterwards, the glass bottle was closed and placed in an oven, and kept reaction for 3 h at 90℃. After naturally cooling to room temperature, the obtained product was treated by centrifugation, repeated washing with deionized water for several times, and then finally dried by freeze-drying. After freeze-drying, a black SNPG nanohybrid (SNPG-50) was obtained. When $(NH_4)_2S$ was not used under otherwise identical conditions, N-undoped sample were prepared, namely as SPG. In addition, for comparison, a series of S, N dual-doped samples with different amounts (0 μL, 25 μL, 75 μL and 100 μL) of MPTS were also prepared. The resultant samples were noted as NPG, SNPG-25, SNPG-75 and SNPG-100, respectively.

Characterization. XRD patterns of resultant products were measured on a Bruker D8 Focus X-ray diffractometer with a Cu Kα X-ray source (40 mA, 40 kV). SEM images were obtained on a Hitachi S-4300 field emission scanning electron microscope operating at 10 kV. TEM images were recorded on a JEOL JEM-2100F transmission electron microscope. Raman spectra were obtained on a Raman spectrometer (Via-Reflex, Renishaw, U.K.) with an incident wavelength of 532 nm. Nitrogen adsorption-desorption measurements were carried out at 77 K using a Quadrasorb SI automate surface area and pore size analyzer. Fourier-transform infrared (FT-IR) spectra were recorded in the range of 300-4000 cm^{-1} at a resolution of 2 cm^{-1} on a Varian Excalibur 3100 spectrometer. X-ray photoelectron spectroscopy (XPS) analysis was performed on an ESCALAB 250Xi (Thermo Fisher Scientific) spectrometer. A Varian 710 ICP-

OES (Varian, USA) and a Plasma Quad 3 ICP-MS (VG, UK) were employed for determining metal ion concentrations. The pH values of solutions were measured using a Five Easy Plus pH meter (Mettler Toledo, FE28).

Adsorption experiments. The aqueous solutions of Hg(II) with different concentrations were obtained by diluting a standard solution with proper amounts of distilled water unless otherwise indicated. The pH levels of the solutions were adjusted by HNO_3 or NaOH aqueous solutions. The Hg(II) concentrations during all experiments were measured by ICP-OES and inductively coupled plasma-mass spectrometry (ICP-MS) for extra low concentrations (≤ppb), , which can identify the metal elements at ppt-ppb levels[2]. All adsorption experiments were performed under ambient conditions.

Hg(II) adsorption kinetics. 50 mg of SNPG-50 was added into a 100 mL Hg(II) solution (initial concentration ~15 ppm) at room temperature, followed by continuous vigorous shaking on a shaker (200 rpm). At predetermined time intervals, aliquots (8 mL) were taken from the mixture, and separated by syringe filter (0.45-μm membrane filter). The supernatants were then analyzed by ICP-OES or ICP-MS. The adsorption efficiency of Hg(II) in solution was calculated by:

$$Removal\ (\%) = \frac{C_0 - C_t}{C_0} \times 100 \tag{S1}$$

where C_0 and C_t (mg L^{-1}) are the initial concentration and the concentration of Hg(II) at time t, respectively. The experimental data were fitted with the pseudo-second-order kinetic model expressed as:

$$\frac{t}{Q_t} = \frac{1}{k_2 Q_e^2} + \frac{t}{Q_e} \tag{S2}$$

where k_2 (g mg^{-1} min^{-1}) is the pseudo-second-order rate constant of adsorption, Q_t (mg g^{-1}) is the amount of Hg(II)adsorbed at time t (min), and Q_e (mg g^{-1}) is the amount of Hg(II)adsorbed at equilibrium.

Hg(II) adsorption isotherms. To calculate the adsorption capacity of SNPG, a series of solutions with 10-500 ppm Hg(II) were employed to conduct isothermal adsorption experiments. 10 mg SNPG was added into 20 mL aqueous solutions with different Hg(II)concentrations. The mixtures were shaken continuously for 24 h, by which time

the adsorption equilibrium was reached. The treated mixtures were separated by syringe filter (0.45-μm membrane filter) and the supernatants were analyzed by ICP-OES to determine the residual Hg(II) concentrations. The adsorbed amount of Hg(II) at equilibrium (Q_e, mg g^{-1}) was calculated using:

$$Q_e = \frac{(C_0 - C_e)}{m} \times V \tag{S3}$$

where C_0 and C_e (mg L^{-1}) are the initial and equilibrium concentrations of Hg(II), respectively. V is the solution volume (L), and m is the amount of used adsorbent (g).

To explore the effect of MPTS content on its adsorption capacity, 10 mg of SNPG prepared with different volumes of MPTS (SNPG-0, SNPG-25, SNPG-50, SNPG-75 and SNPG-100) were added in 20 mL of solutions with different Hg(II) concentrations. For evaluating the pH effect on Hg(II) uptake, 20 mL aqueous solutions of Hg(II) (initial concentration ~10 ppm) were treated by 10 mg SNPG-50 at various pH values (2-10) for 24 h.

Selectivity test experiments. A pH 4 solution consisting of Hg(II), Pb(II), Cu(II), Cr(III), Cd(II), Ni(II), Mn(II), K(I) and Na(I) (each ~10 ppm) was used for selectivity studies. The metal ions were used as their nitrate salts. At the pH value of 4, the mixed metal ions are stable.[3] 10 mg SNPG-50 and 20 mL mixture solution were used, with 24 h contact, followed by similar post-processing as that described above.

The separation factor ($SF_{Hg/M}$), indicating the relative selectivity of adsorbent to Hg(II) and other metal ions[4], were also investigated by the following equation:

$$SF_{Hg/M} = \frac{K_{d(Hg)}}{K_{d(M)}} \tag{S4}$$

$$K_d = \frac{C_0 - C_e}{C_e} \times \frac{V}{m} \tag{S5}$$

where K_d is the distribution coefficient, C_0 and C_e (mg L^{-1}) represent the initial concentration and final equilibrium concentration of Hg(II), respectively. V is the volume of the treated solution (mL) and m is the mass of adsorbent used (g).

Equilibrium models

Langmuir isotherm model:

The Langmuir isotherm model can display the monolayer molecule adsorption onto homogeneous active sites of adsorbents. The Langmuir model is expressed linearly as:

$$\frac{C_e}{Q_e} = C_e\frac{1}{Q_{max}} + \frac{1}{K_L Q_{max}} \quad \text{(S6)}$$

where Q_{max} (the maximum Hg(II) adsorption capacity, mg g^{-1}) and K_L (the Langmuir constant, L mg^{-1}) can be obtained by plotting C_e/Q_e *versus* C_e. C_e and Q_e are the Hg(II) concentration and adsorbed Hg(II) amount at equilibrium, respectively.

Freundlich isotherm model:

The Freundlich isotherm model depicts the homogeneous active sites on the adsorbent surface and is always used to describe the multilayer adsorption. The Freundlich model is expressed linearly as:

$$LnQ_e = LnK_F + \frac{1}{n}LnC_e \quad \text{(S7)}$$

where K_F (the Langmuir constant, L mg^{-1}) and n can be obtained by plotting LnQ_e *versus* LnC_e. 1/n represents the Freundlich adsorption constant related with adsorption intensity.

Temkin isotherm model:

The Temkin isotherm model describes some indirect adsorbent-adsorbate interaction in the adsorption process. The Temkin equation:

$$Q_e = BLnC_e + BLnK_T \quad \text{(S8)}$$

where K_t (the Temkin constant, L mg^{-1}) and B (a constant related to heat of adsorption) can be obtained by plotting Q_e *versus* LnC_e.

Henry isotherm model:

$$Q_e = K_H C_e \quad \text{(S9)}$$

where K_H is the Henry constants related to the adsorption capacity.

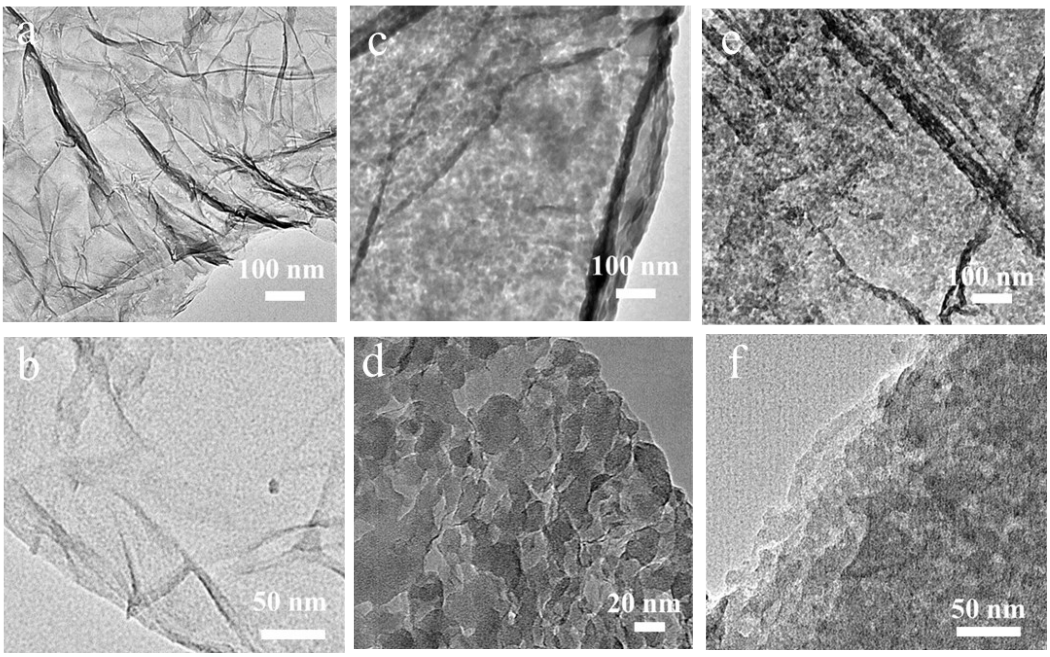

Fig. S1 TEM and HRTEM images of NPG (a, b), SNPG-25 (c, d) and SNPG-50 (e, f).

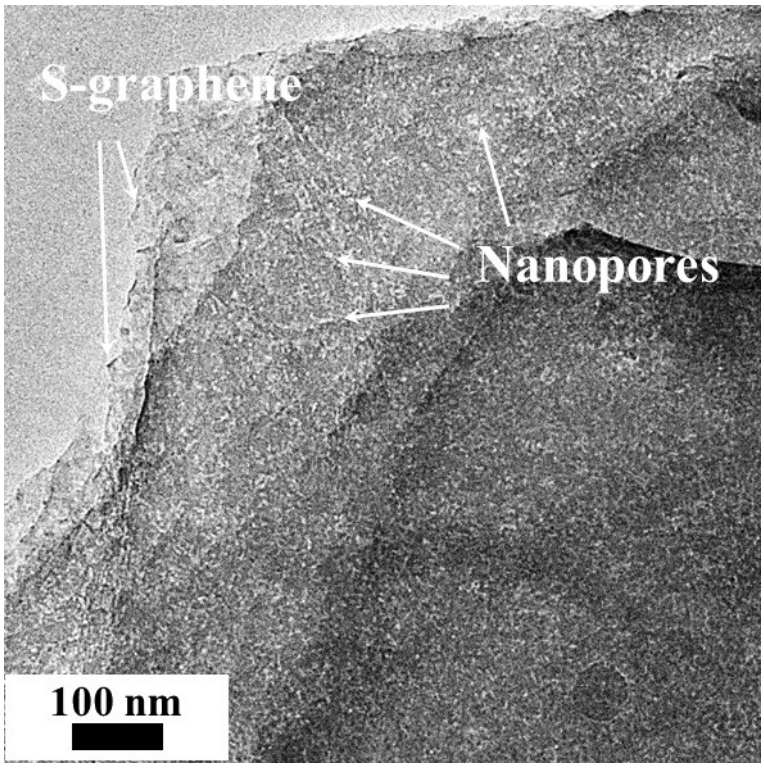

Fig. S2 TEM image of SPG prepared without $(NH_4)_2S$.

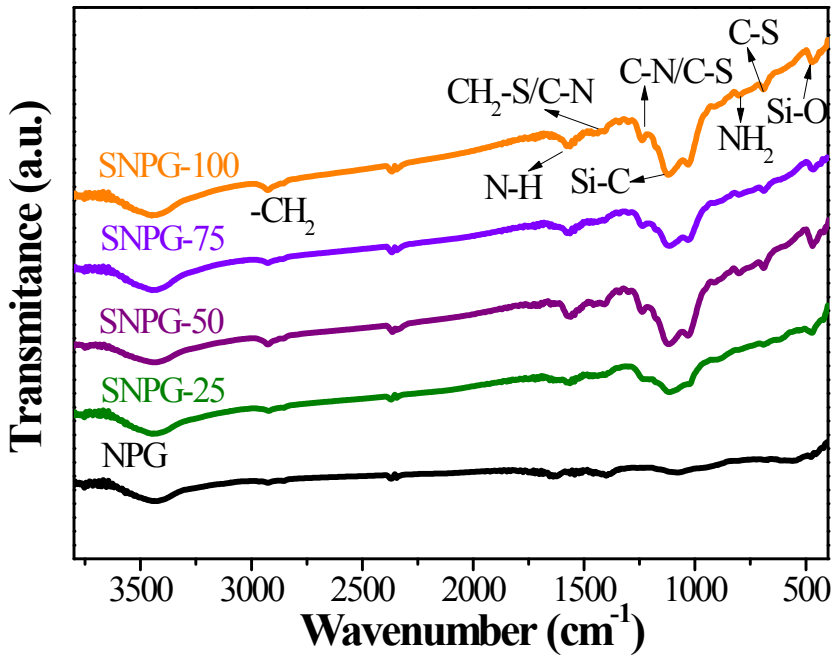

Fig. S3 FT-IR spectra of NPG, SNPG-25, SNPG-50, SNPG-75 and SNPG-100.

Table S1. Contents of C, O, Si, N and S atoms in samples.

Sample	Content (at. %)				
	C	O	Si	N	S
NPG	86.66	9.79	0	1.08	2.47
SPG	63.54	23.13	7.80	0	5.52
SNPG	56.59	20.98	11.42	0.85	10.15

Table S2. Comparison of Hg(II) adsorption capacity of SNPG with other reported adsorbents.

Adsorbent	S_{BET} (m^2 g^{-1})	C_0 (mgL^{-1})	Adsorbent amount (mg L^{-1})	Q_e (mg g^{-1})	Ref.
Thiol functionalized silica	951.5	196.8	10000	19.6	5
Sulfur-functionalized silica	622.8	50	1000	47.5	6
3-Aminopyrazole modified GO	-	20	333.3	227.3	7
MGO-PAMAM	40.9	100	500	113.7	8
Thiol functionalized GO	106.0	-	-	450(Q_{max})	9
PA-induced 3D graphene	201.2	-	-	361(Q_{max})	10
*p*S-rGO	449.4	500	500	829	11
CBAP(AET)	422	-	1000	232	12
SNPG	153.7	204	500	803	This work

Table S3. Langmuir, Freundlich, Temkin and Henry model parameters for Hg(II) adsorption with SNPG.

Model	K(L mg^{-1})	n	B	Q_{max} (mg g^{-1})	R^2
Langmuir	0.05	-	-	909	0.9709
Freundlich	48.29	1.48	-	-	0.9211
Temkin	1.50	-	137.62	-	0.9395
Henry	8.83	-	-	-	0.8435

Table S4 Absolute hardness and radius values for some common cations.

Cation	Absolute hardness[a]	Radius[b] (Å)
Na(I)	21.1 (hard)	1.02
K(I)	13.6 (hard)	1.38
Mg(II)	32.5 (hard)	0.72
Mn(II)	9.3 (hard)	0.83
Ni(II)	8.5 (borderline)	0.69
Cd(II)	10.3 (hard)	0.95
Cr(III)	9.1 (hard)	0.62
Cu(II)	8.3 (borderline)	0.73
Pb(II)	8.5 (borderline)	1.19
Hg(II)	7.7 (soft)	1.02

[a] from the literature by Pearson, R.G., et al [13].

[b] from the literature by Shannon, R. D.[14]

References

1. H. Tian, Y. Cao, J. Sun and J. He, *RSC Adv.*, 2017, **7**, 46536-46544.
2. Z. Hassanzadeh Fard, S. M. Islam and M. G. Kanatzidis, *Chem. Mater.*, 2015, **27**, 6189-6192.
3. L. Rong, Z. Zhu, B. Wang, Z. Mao, H. Xu, L. Zhang, Y. Zhong and X. Sui, *Cellulose*, 2018, **25**, 3025-3035.
4. H. Asiabi, Y. Yamini, M. Shamsayei, K. Molaei and M. Shamsipur, *J. Hazard. Mater.*, 2018, **357**, 217-225.
5. H. Chen and J. He, *Dalton Trans.*, 2009, **33**, 6651-6655.
6. N. Saman, K. Johari and H. Mat, *Micropor. Mesopor. Mater.* 2014, **194**, 38-45.
7. M. Alimohammady, M. Jahangiri, F. Kiani and H. Tahermansouri, *New J. Chem.* 2017, **41**, 8905-8919.
8. Y. X. Ma, D. Xing, W. J. Shao, X. Y. Du and P. Q. La, *J. Colloid Interf. Sci.*, 2017, **505**, 352-363.
9. S. Xia, Y. Huang, J. Tang and L. Wang, *Environ. Sci. Pollut. Res. Int.*, 2019, **26**, 8709-8720.
10. B. Tan, H. Zhao, Y. Zhang, X. Quan, Z. He, W. Zheng and B. Shi, *J. Colloid Interf. Sci.*, 2018, **512**, 853-861.
11. B. Manna and C. R. Raj, *ACS Sustain. Chem. Eng.*, 2018, **6**, 6175-6182.
12. S. Ravi, P. Puthiaraj, K. H. Row, D.-W. Park and W.-S. Ahn, *Ind. Eng. Chem. Res.*, 2017, **56**, 10174-10182.
13. R. G. Pearson, *Inorg. Chem.*, 1988, **27**, 734-740.
14. R. D. Shannon, *Acta Cryst.*, 1976, **32**, 751-767.